Optimization of a simultaneous dual-isotope 201Tl/123I-MIBG myocardial SPECT imaging protocol with a CZT camera for trigger zone assessment after myocardial infarction for routine clinical settings: Are delayed acquisition and scatter correction necessary?

Emmanuel d'Estanque, Christophe Hédon, Benoît Lattuca, Aurélie Bourdon, Meriem Benkiran, Aurélie Verd, François Roubille, Denis Mariano-Goulart

Optimization of a simultaneous dual-isotope ^{201}Tl/^{123}I-MIBG myocardial SPECT imaging protocol with a CZT camera for trigger zone assessment after myocardial infarction for routine clinical settings: Are delayed acquisition and scatter correction necessary?

Emmanuel D'estanque, MD,[a] Christophe Hedon, MD,[b,c] Benoît Lattuca, MD,[b] Aurélie Bourdon, MD,[a] Meriem Benkiran, MD,[a] Aurélie Verd, MD,[a] François Roubille, MD, PhD,[b,c] and Denis Mariano-Goulart, MD, PhD[a,c]

[a] Nuclear Medicine Department, Montpellier University Hospital, Montpellier Cedex 5, France
[b] Cardiology Department, Montpellier University Hospital, Montpellier, France
[c] U1046 INSERM, UMR9214 CNRS, Montpellier University Hospital, Montpellier, France

Background. **Dual-isotope ^{201}Tl/^{123}I-MIBG SPECT can assess trigger zones (dysfunctions in the autonomic nervous system located in areas of viable myocardium) that are substrate for ventricular arrhythmias after STEMI. This study evaluated the necessity of delayed acquisition and scatter correction for dual-isotope ^{201}Tl/^{123}I-MIBG SPECT studies with a CZT camera to identify trigger zones after revascularization in patients with STEMI in routine clinical settings.**

Methods. **Sixty-nine patients were prospectively enrolled after revascularization to undergo ^{201}Tl/^{123}I-MIBG SPECT using a CZT camera (Discovery NM 530c, GE). The first acquisition was a single thallium study (before MIBG administration); the second and the third were early and late dual-isotope studies. We compared the scatter-uncorrected and scatter-corrected (TEW method) thallium studies with the results of magnetic resonance imaging or transthoracic echography (reference standard) to diagnose myocardial necrosis.**

Results. **Summed rest scores (SRS) were significantly higher in the delayed MIBG studies than the early MIBG studies. SRS and necrosis surface were significantly higher in the delayed thallium studies with scatter correction than without scatter correction, leading to less trigger zone diagnosis for the scatter-corrected studies. Compared with the scatter-uncorrected studies, the late thallium scatter-corrected studies provided the best diagnostic values for myocardial necrosis assessment.**

Conclusions. **Delayed acquisitions and scatter-corrected dual-isotope ^{201}Tl/^{123}I-MIBG SPECT acquisitions provide an improved evaluation of trigger zones in routine clinical settings after revascularization for STEMI.**

Key Words: Trigger zone • MIBG • myocardial infarction • scatter correction • cardiac SPECT

Abbreviations

CZT	Cadmium zinc telluride
H/M	Heart to mediastinum
HF	Heart failure
MI	Myocardial infarction
MIBG	Methyliodobenzylguanidine
MMA	Maximal myocardial activity
MRI	Magnetic resonance imaging
MSA	Mean segmental activity
SCD	Sudden cardiac death
SPECT	Single-photon emission computed tomography
SRS	Summed rest score
STEMI	ST-elevation myocardial infarction
TEW	Triple energy window
TSS	Trigger summed score
TTE	Transthoracic echography
VA	Ventricular arrhythmia

INTRODUCTION

Ischemic cardiomyopathy is widespread and may cause such undesirable cardiac events as sudden cardiac death (SCD) secondary to ventricular arrhythmia (VA).

After myocardial infarction (MI), regional sympathetic denervation as assessed by ^{123}I-metaiodobenzylguanidine (^{123}I-MIBG) exceeds the extent of the perfusion defect,[1] probably because of increased sensitivity of neural tissue to hypoxia. Evidence indicates that comparing cardiac sympathetic innervation, using ^{123}I-MIBG single-photon emission computed tomography (SPECT), and myocardial viability is of potential interest to assess the risk of VA after MI.[2-5] This evaluation might provide a tool for individual risk stratification for SCD.

MIBG is a norepinephrine analogue that has been widely described to be a sensitive indicator of cardiac sympathetic neuronal function integrity.[6] Trigger zones are defined as areas of autonomic nervous system dysfunction in viable myocardium that may contribute to the genesis of VA.[7]

For at least two decades, indexes derived from the analysis of the ^{123}I-MIBG kinetics used in planar imaging, such as the heart-to-mediastinum (H/M) ratio and the myocardial washout rate,[8-10] have been associated with arrhythmic events and cardiac death, especially in cases of chronic heart failure (HF).[5,8,11-15] Although these parameters are in routine use, they provide only an overall picture of cardiac adrenergic activity but cannot determine regional differences in myocardial innervation that may characterize specific cardiac pathologies, especially ischemic heart disease. SPECT allows the description of regional abnormalities in cardiac innervation, typically quantified from summed visual scores on polar plots.[5]

Most of the recent studies[4,5,16,17] on myocardial viability and sympathetic innervation have used sequential or simultaneous dual-isotope ^{99m}Tc/^{123}I SPECT imaging. This technique does not require image registration, reduces the time of the acquisition protocol, improves patient comfort, and is compatible with trigger zone assessment in routine clinical settings.

Cadmium-zinc-telluride (CZT) solid-state detectors were recently introduced into the field of myocardial perfusion imaging. In this camera, the conventional sodium iodide crystals have been replaced by CZT semiconductors, which directly convert radiation into electric signals. Thus, dedicated cardiac CZT cameras offer greater sensitivity and better energy resolution.[18,19] In addition to the longer acquisition time, simultaneous dual-isotope SPECT imaging with Anger cameras is hampered by poor image quality due to the crosstalk of photons from one radionuclide to the other radionuclide's photopeak. These new CZT cameras are likely to overcome, at least partially, these two limitations of conventional gamma cameras for dual-isotope imaging.

To assess trigger zones using simultaneous ^{201}Tl/^{123}I-MIBG imaging, a strict limitation of ^{123}I crosstalk in the thallium photopeak is of paramount importance. With dual-isotope ^{201}Tl/^{123}I-MIBG imaging, the decrease in contrast in the thallium images may result in an overestimation of myocardium viability and hence an overestimation of the myocardium surface with trigger zones. Despite the increased energy resolution, the need for scatter correction with CZT cameras remains uncertain for trigger zone assessment.

The primary endpoint of our study was to assess the need for a scatter correction for dual-isotope ^{201}Tl/^{123}I-MIBG SPECT studies with a dedicated cardiac CZT camera.

The secondary endpoint was to evaluate the need for ^{123}I-MIBG delayed acquisition for identification of sympathetic cardiac denervation.

MATERIALS AND METHODS

Patients

All patients were prospectively recruited from the intensive care unit of the cardiology department of Montpellier University Hospital between January 2014 and September 2014. The institutional review board approved this study, and the requirement of informed consent was waived. During this period, all patients with ST-elevation myocardial infarction (STEMI) were referred to the intensive care unit of the cardiology department for primary percutaneous coronary

intervention. After appropriate therapy (coronary revascularization leading to TIMI 3 flow and medical treatment), all patients were systematically considered for myocardial sympathetic innervation and perfusion SPECT. Exclusion criteria included a previous history of MI, HF, dilated or hypertrophic cardiomyopathy, Parkinson's disease or treated psychiatric diseases. Sixty-nine patients were prospectively enrolled.

SPECT studies

All SPECT studies were performed (12 ± 8 days after MI) with patients in the supine position and arms over the head, using a cardiac dedicated multi-pinhole CZT camera (Discovery NM 530c, GE Healthcare, Tirat Camel, Israel). Myocardial rest perfusion and sympathetic innervation SPECT were performed with the following acquisition parameters: list mode, 32 × 32 matrix size, pixel size: 4 mm. Scatter-uncorrected projections were extracted from list mode files using a Xeleris workstation (GE Healthcare) with windows centered at 67 keV ± 10% for ^{201}Tl and 159 keV ± 10% for ^{123}I.

The first SPECT study was a single-isotope thallium acquisition. The second and third acquisitions were dual-isotope SPECT studies. The examination time was 6 minutes for each. In cases of digestive or motion artifacts or uncorrected cardiac alignment, the acquisitions were repeated to ensure the best image quality and an interpretable examination. The design of the sequential acquisitions is given in Figure 1.

^{201}Tl SPECT. Rest myocardial perfusion SPECT studies were performed 10 minutes (Tl1), 26 minutes (Tl2), and 3 hours 32 minutes (Tl3) after intravenous administration of thallium chloride (92 MBq). The last two acquisitions were obtained after MIBG administration.

Tl1 and Tl2 studied the rest myocardial perfusion while Tl3 studied the myocardial viability.

^{123}I-MIBG SPECT. In line with the guidelines,[10] thyroid blockade was achieved by oral administration of 130 mg of potassium iodine 1 hour before MIBG administration.

Rest myocardial sympathetic innervation SPECT studies were performed 10 minutes (MIBG 1) and 3 hours (MIBG 3) after intravenous administration of ^{123}I-MIBG (Adreview®, 185 MBq) performed at the end of the first thallium acquisition.

Data reconstruction. A regularized OSL-green algorithm was used to reconstruct the projection data following the manufacturer's specifications (30 iterations, $\alpha = \beta = 0.4$, Butterworth post-filter with order 10 and cutoff frequency 0.4/cm), and horizontal short-axis and vertical long-axis sections were obtained. The reconstructed slices were analyzed using Quantitative Perfusion Spect software® (Cedars-Sinai).

Scatter correction

All projections were first reconstructed without scatter correction. Tl3 projections were then reconstructed with scatter correction (Tl3c) using the triple energy window (TEW) method.[20-22] The chosen energy windows were: 70 keV ± 12% for the main window ($W = 8.4$ keV), and 60.1 keV ± 2% ($w_1 = 1.2$ keV) and 79.9 keV ± 2% ($w_2 = 1.6$ keV) for the two subwindows. The scatter correction was performed with the ''Load to new'' application on the Xeleris workstation (GE Healthcare). The aim of this scatter correction was to eliminate the low-energy scattered photons from ^{123}I from the main energy window of ^{201}Tl. Tl3c projections were obtained with the following formula[21] where Tl^l and Tl^h are defined as the photon counts in the low- and high-energy subwindows, respectively:

$$Tl_{3c} = Tl_3 - \frac{W}{w_1 + w_2}(Tl^l + Tl^h) = Tl_3 - 3.(Tl^l + Tl^h)$$

No scatter correction has been performed for the 123I-MIBG scans.

Image analysis

Two experienced nuclear medicine physicians unaware of the clinical information analyzed the images in terms of defect number and severity. Myocardial perfusion and innervation bull's eye images were divided into 17 segmental regions.[23,24] Each region was automatically scored independently using a five-point model depending on the mean segmental activity (MSA) expressed as a ratio of the maximal myocardial activity (0: MSA ≥ 70%; 1: 50 ≤ MSA < 70%; 2: 30 ≤ MSA < 50%; 3: 10 ≤ MSA < 30%; 4: MSA < 10%). Necrosis inside a segment was considered significant if the mean activity in the segment was below 50% of the maximal myocardial activity (MMA) in perfusion or viability images (Tl1, Tl3, and Tl3c necrosis percentages). A trigger zone inside a segment was considered if the mean activity in the segment was below 50% of the MMA in innervation images but over 50% of MMA in viability images (Tl3). The 17 segmental scores were summed using the rest perfusion and viability

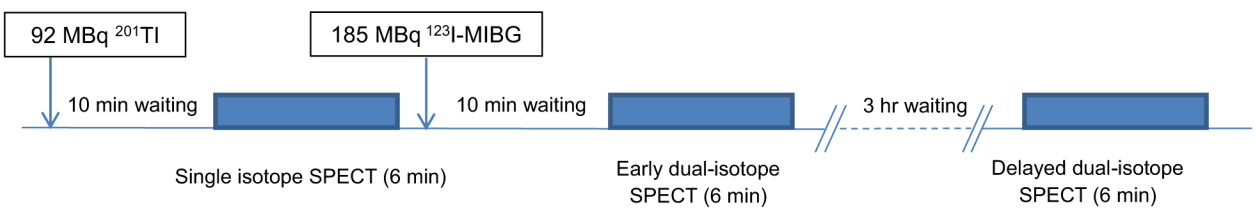

Figure 1. Imaging study protocol. One-day dual-isotope protocol for trigger zone assessment after STEMI. The first acquisition is a single-isotope SPECT, whereas the second and the third are dual isotope.

studies to derive perfusion summed rest scores (SRS Tl1, SRS Tl2, SRS Tl3, and SRS Tl3c with scatter correction) and using the rest innervation studies to derive innervation summed rest scores (SRS MIBG 1 and SRS MIBG 3). Trigger summed scores (TSS) were evaluated by summing from among the 17 segmental scores in the late innervation images (MIBG 3) those scores corresponding to viable myocardium on rest dual-isotope thallium images (TSS1) or on viability studies (TSS 3 and TSS 3c with scatter correction). %TSS values represent the percentage of myocardial surface with viability and impaired innervation.

Cardiovascular magnetic resonance imaging/transthoracic echocardiography

All patients were screened just after appropriate coronary revascularization with cardiovascular magnetic resonance imaging (MRI) (kinetic, thickness and perfusion with late gadolinium enhancement technique of all the myocardium walls analysis) and/or transthoracic echocardiography (TTE) (kinetic and systolic thickening analysis in multiple views) to assess the extent of myocardial necrosis and to estimate left ventricular function. To determine the most accurate myocardial perfusion SPECT study (scatter-corrected or uncorrected), we evaluated the diagnostic values of each ^{201}Tl SPECT study (Tl1, Tl3, and Tl3c) for myocardial necrosis assessment in comparison with MRI (or TTE when MRI was unavailable), which is the reference standard. Grouping together the 17 segments,[23] we divided the left ventricular myocardium into three main regions corresponding to the three coronary artery territories: anterior-septal-apical, lateral, and inferior. Then, we compared the results of the TTE, MRI, and Tl studies (Tl1, Tl3 and Tl3c) region by region for each patient.

Statistical analysis

Continuous variables are expressed as mean ± standard deviation, while categorical variables are presented as percentages.

The distributions of the clinical data are characterized as mean ± standard deviation.

The values of summed rest scores and trigger summed scores were compared with the Student *t* test.

Tl1, Tl3, and Tl3c SPECT studies were calculated for diagnostic value in comparison with MRI (or TTE when no MRI was available).

$P < 0.05$ was considered a statistically significant difference.

Statistical analyses were performed with GraphPad Prism software (version 6.0, La Jolla, CA, USA).

RESULTS

All 69 patients (17 women, 52 men, age 59 ± 13 years) underwent the three SPECT studies.

Patient baseline characteristics are summarized in Table 1. The mean left ventricular ejection fraction was 48% ± 8.2. Only 8 patients presented no necrosis (based on MRI or TTE). Medication consisted of the standard recommended treatment for coronary ischemic disease (antiplatelet agents, beta-blockers or calcic channel blockers, angiotensin-converting enzyme inhibitors and statin).

All patients but one presented trigger zones corresponding to 30% ± 20 [0 to 81%] and 37% ± 18 [0 to 71%] of the surface of the left ventricular myocardium with and without scatter correction, respectively.

Without scatter correction

The variables of myocardial perfusion and ^{123}I-MIBG imaging without scatter correction are shown in Table 2. The crosstalk of ^{123}I in the rest perfusion images induced a significant change in SRS for Tl2 and Tl3 versus Tl1 ($P < 0.0001$). Moreover, no significant changes in SRS were found between early and late thallium images in these patients whose critical coronary lesions had been recently treated (Tl1 and Tl2 versus Tl3; $P < 0.0001$).

SRS MIBG were statistically higher with the delayed MIBG study than the early MIBG study ($P < 0.0001$). Thus, TSS were statistically higher considering late thallium and MIBG dual-isotope acquisitions ($P < 0.0001$).

With scatter correction

The variables of myocardial perfusion and TSS with scatter correction are shown in Table 3. Mean values of perfusion SRS and necrosis surface assessed with Tl3c were statistically higher than in the studies without scatter correction ($P < 0.0001$). Accordingly, there were significantly less trigger zones in the scatter-corrected studies than in the uncorrected studies (TSS 3c:14 ± 7 and %TSS 3c: 30% ± 20, $P < 0.0001$).

Figure 2 shows an example of scatter-uncorrected Tl3 (A) and scatter-corrected Tl3c (B) rest perfusion and sympathetic innervation (C) SPECT polar plot representations.

Diagnostic values

Thirty-three patients were screened by MRI and 36 patients by TTE. The diagnostic values of the SPECT studies are shown in Table 4.

The ^{201}Tl dual-isotope scatter-corrected SPECT studies (Tl3c) had superior sensitivity and negative predictive value with similar specificity and positive predictive value for myocardial necrosis assessment in comparison with the ^{201}Tl single-isotope (Tl1) and ^{201}Tl

Table 1. Baseline characteristics of the study population ($n = 69$)

Characteristics	Values
Sex*	
Male	52/69 (75)
Female	17/69 (25)
Age†	59 ± 13
Body mass index†	26 ± 3
CVRF†	2 ± 1
Diabetes*	11/69 (16)
Hypertension*	33/69 (47)
Hypercholesterolemia*	24/69 (34)
Smoking*	35/69 (50)
Family history of CAD*	8/69 (11)
High sensitive Troponin T†	
Admission	2214 ± 3887
Peak	5672 ± 5208
Timing of revascularization from onset of symptoms†	3.6 h ± 2.5
Sites of revascularization	
Interventricular artery and diagonal branches	39
Circumflex/marginal arteries	14
Right coronary and posterior descending arteries	24
LVEF†	48% ± 8.2
Necrosis‡	
None	3/5
Anterior	20/14
Lateral	2/5
Inferior	8/10
Medication use at the time of the SPECT studies*	
Beta-blocker	68/69 (98)
Amiodarone	3/69 (4)
ACE-I/ATII antagonist	67/69 (97)
Calcium channel blockers	6/69 (8.5)

* Reported as numbers of patients from total and as percentage in parentheses
† Mean ± SD
‡ Numbers of lesions detected by magnetic resonance imaging/transthoracic echography
ACE-I angiotensin-converting enzyme inhibitor, *AT* angiotensin, *CAD* coronary artery disease, *CVRF* cardiovascular risk factor, *LVEF* left ventricular ejection fraction

dual-isotope (Tl3) SPECT studies, both without scatter correction.

DISCUSSION

The main findings of the study can be summarized as follows. Despite increased energy resolution with a dedicated cardiac CZT camera, scatter correction is necessary in simultaneous dual-isotope ^{201}Tl/^{123}I-MIBG myocardial imaging. The dual-isotope combination ^{201}Tl scatter-corrected/^{123}I-MIBG scatter-uncorrected SPECT acquisition provides the best evaluation of myocardial viability and sympathetic innervation. Moreover, the best mapping of segmental myocardial sympathetic denervation is obtained with delayed ^{123}I-MIBG SPECT acquisition. In our studies early acquisitions did not help define trigger zones.

Table 2. Variables of myocardial perfusion and 123-I MIBG imaging without scatter correction

Myocardial perfusion (thallium)	
SRS Tl1	10 ± 5
SRS Tl2	5 ± 4
SRS Tl3	6 ± 4
Necrosis Tl1 (%)	9 ± 12
Necrosis Tl3 (%)	5 ± 7
123I-MIBG	
SRS MIBG 1	14 ± 6
SRS MIBG 3	21 ± 7
TSS 1	17 ± 6 [4–33]
%TSS 1†	32 ± 18 [0–81]
TSS 3	19 ± 6 [5–30]
%TSS 3†	37 ± 18 [0–71]

Reported as mean value ± standard deviation [min–max]
† %TSS are percentages of myocardial surface with viability and impaired innervation
SRS summed rest scores, *TSS* trigger summed scores

Table 3. Variables of myocardial perfusion and 123-I MIBG imaging with scatter correction

Myocardial perfusion (thallium)	
SRS Tl3c	14 ± 6
Necrosis Tl3c (%)	19 ± 17
123I-MIBG	
TSS 3c	14 ± 7 [2–30]
%TSS 3c†	30 ± 20 [0–81]

Reported as mean value ± standard deviation [min–max]
† %TSS are percentages of myocardial surface with viability and impaired innervation
SRS summed rest scores, *TSS* trigger summed scores

Scatter correction and CZT camera

Simultaneous dual-isotope imaging has several potential advantages, including reduced patient discomfort and lower acquisition time. More importantly, it produces images that are perfectly registered in space and time, which is particularly interesting for assessing

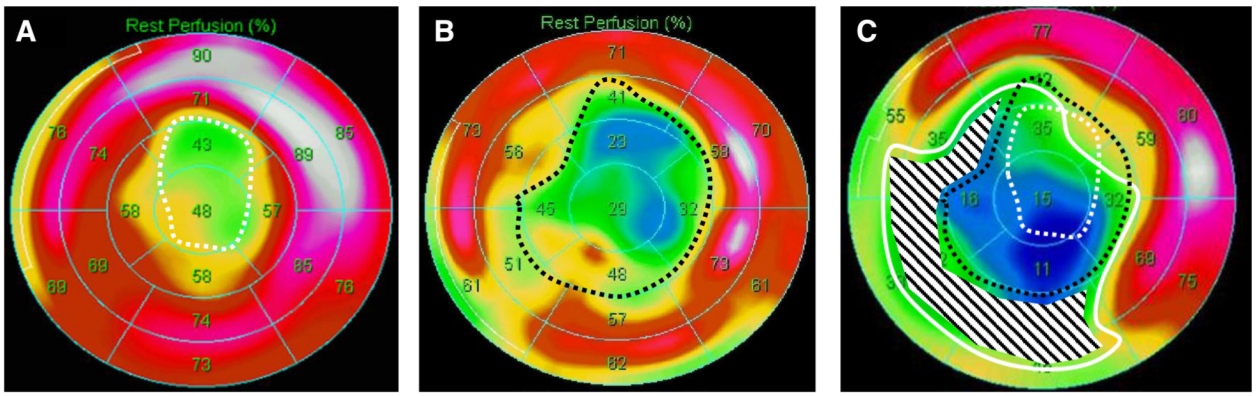

Figure 2. Example of scatter-uncorrected Tl3 (**A**) and scatter-corrected Tl3c (**B**) rest perfusion and sympathetic innervation (**C**) SPECT polar plot representations. The *white- and black-dotted lines* represent, respectively, left ventricular myocardium surface without viability on scatter-uncorrected and scatter-corrected polar plot representations. The *white line* represents left ventricular myocardium surface with impaired sympathetic innervation. The *black ray area* represents the trigger zone area (viable but with impaired innervation myocardium).

Table 4. Diagnostic values of SPECT in myocardial necrosis at per-patient-based assessment with MRI/TTE as the reference standard

	Tl1	Tl3	Tl3c
Sensitivity*	52 [35-69]	37 [17.3-56.7]	72 [59-85]
Specificity*	92 [87.4-96.6]	95 [91.3-98.7]	91 [86.1-95.9]
Positive predictive value*	75 [60.2-89.8]	77 [59.8-94.2]	78 [66-90]
Negative predictive value*	82 [75.5-88.5]	77 [69.9-84.1]	88 [82.4-93.6]

* Reported as value in percentage and 95% confidence interval in parentheses

trigger zones. Nevertheless, scatter correction appears to be very important because of the spillover effects caused by down-scatter from the higher energy emission detected in the lower energy photopeak.

In trigger zone assessment without scatter correction, ^{123}I down-scatter detected in the thallium photopeak may mask myocardial necrosis and thus leads to an overestimation of the trigger zone.

The correction of scatter improves image quality and quantification accuracy with conventional NaI-based gamma cameras. To the best of our knowledge, however, no recent study has reported the interest of scatter correction in dual-isotope cardiac SPECT imaging for trigger zone assessment with CZT cameras, which provide much better energy resolution than Anger cameras.

Scatter causes blurred and hazy projections, reduces reconstructed contrast, and introduces significant uncertainty into the quantification of the underlying activity distribution.[25] In cardiac SPECT, the use of accurate scatter correction models improves not only diagnostic accuracy[26] but also quantitative accuracy, the signal-to-noise ratio and the detectability of small defects.[27]

The TEW approach [20] we used is the most effective and simplest validated method in routine clinical settings for scatter correction, providing an estimate of the scatter contribution that degrades the photopeak window image independently of the distribution of activity.[28] It involves subtraction of the scatter estimated pixel by pixel from the photopeak projection image. Ichihara et al[21] and Yang et al[22] applied this method in dual-isotope ^{201}Tl/^{123}I SPECT with conventional cameras. The main disadvantage of this method is the noise amplification that arises due to acquiring relatively low counts in the necessarily narrow scatter windows, accentuated by pixel-by-pixel subtraction. Nevertheless, this drawback is less problematic with CZT cameras because of their high sensitivity compared with the Anger detector. Scatter rays may also be modeled in the core of iterative reconstruction algorithms using Monte Carlo simulations, but these solutions, which have been

extensively used in positron emission tomography imaging, are less common with SPECT.[27,29]

The model is further complicated in the case of solid-state detectors because of a low-energy component due to incomplete charge detection in the detector, which cannot easily be separated from a lower energy peak.[28] Although this incomplete charge collection and inter-pixel scatter may impair the performances of TEW methods, adjustments of these methods for CZT detectors[30-32] are not widely available in routine clinical settings, so TEW algorithms are still widely used in dual-isotope imaging.

Until now, guidelines have made no recommendations about scatter correction in simultaneous dual-isotope ^{201}Tl/^{123}I myocardial imaging, particularly with CZT cameras. Nevertheless, recent studies suggest that scatter correction could improve the dual-isotope myocardial imaging with CZT cameras. Rouzet et al[33] evaluated the clinical application of simultaneous imaging with a cardiac CZT camera with a multiple energy windows model processed for scatter correction. The dual-isotope acquisition yielded results similar to those obtained sequentially with conventional cameras. Pourmoghaddas et al[32] recently suggested that scatter correction improves the concordance between the CZT camera and the conventional camera in SPECT myocardial perfusion imaging. Ben-Haim et al[34] validated a dual-radionuclide ^{201}Tl/^{99m}Tc myocardial perfusion imaging protocol with scatter correction with a D-SPECT camera.

Myocardial infarction and sympathetic denervation

Most of the studies that have evaluated ^{123}I-MIBG as an imaging tool to predict VA in the context of HF and ischemic disease compared myocardial rest perfusion and sympathetic innervation.[1,2,4,5,8,34] As nerve tissue is more sensitive to ischemia than the cardiomyocytes,[1] the regional impairment in sympathetic tone is likely to exceed the area of altered myocardial perfusion[1,3,35] and seems to be associated with the presence and extent of myocardial oedema.[3] Thus, as in HF, ^{123}I-MIBG SPECT could be used in clinical routine to stratify patients after MI into a low-risk or high-risk group for arrhythmias. The quantification with the 17-segment model[24] in ^{123}I-MIBG SPECT permits a comparison with myocardial perfusion SPECT and cardiac MRI to assess innervation/perfusion mismatch areas defined as trigger zones, a substrate for post-infarction ventricular arrhythmias in MI patients.

The quantification of the magnitude of these automatic trigger zones could become a new prognostic factor in the management of MI and the clinical significance has to be investigated.

Study limitations

This study has limitations that should be acknowledged. First, we did not have MRI data for every patient. This was mainly due to the difficulty of performing cardiovascular MRI during the patients' initial hospitalization, as the study was designed to conform to routine situations in an intensive care unit.

Second, it is unclear whether the observed differences between scatter-corrected and scatter-uncorrected SPECT are clinically relevant. Although statistically significant, the differences between scatter-corrected and scatter-uncorrected SRS and TSS must be analyzed within the set of clinical circumstances. Further studies are required to evaluate the clinical value of dual-isotope ^{201}Tl/^{123}I-MIBG imaging with a CZT camera to screen for patients at high risk of clinical outcomes like arrhythmia after revascularization in STEMI.

Several drugs are known or assumed to interfere with organ MIBG uptake, including beta-blockers, angiotensin-converting enzyme inhibitors, and angiotensin receptor blockers.[10] Most of the enrolled patients were treated daily with these drugs. However, many studies have demonstrated that cardiac MIBG imaging can be performed in patients with optimum medical therapy.[15,36] The characteristics of our study patients were similar to those of patients routinely admitted for suspicion of MI. Therefore, our results reflect the feasibility of sympathetic denervation SPECT assessment in routine conditions.

NEW KNOWLEDGE GAINED

Despite an increased resolution in energy, using a scatter correction with CZT camera is needed for dual-isotope ^{201}Tl/^{123}I-MIBG SPECT protocols. This correction improves the accuracy and the quantification of myocardial SPECT.

CONCLUSIONS

Scatter correction is necessary in myocardial simultaneous dual-isotope ^{201}Tl/^{123}I-MIBG imaging with solid-state dedicated cardiac CZT cameras. The scatter-corrected dual-isotope ^{201}Tl/^{123}I-MIBG SPECT acquisition provides an improved evaluation of myocardial perfusion and sympathetic innervation.

To obtain the best mapping of segmental myocardial sympathetic denervation, a delayed ^{123}I-MIBG SPECT acquisition is required.

Disclosures

The authors have indicated that they have no financial conflict of interest.

References

1. Matsunari I, Schricke U, Bengel FM, Haase H-U, Barthel P, Schmidt G, et al. Extent of cardiac sympathetic neuronal damage is determined by the area of ischemia in patients with acute coronary syndromes. Circulation 2000;101:2579–85.
2. Bax JJ, Kraft O, Buxton AE, Fjeld JG, Pařízek P, Agostini D, et al. 123I-mIBG scintigraphy to predict inducibility of ventricular arrhythmias on cardiac electrophysiology testing a prospective multicenter pilot study. Circ Cardiovasc Imaging 2008;1:131–40.
3. Gimelli A, Masci PG, Liga R, Grigoratos C, Pasanisi EM, Lombardi M, et al. Regional heterogeneity in cardiac sympathetic innervation in acute myocardial infarction: relationship with myocardial oedema on magnetic resonance. Eur J Nucl Med Mol Imaging 2014;41:1692–4.
4. Gimelli A, Liga R, Giorgetti A, Genovesi D, Marzullo P. Assessment of myocardial adrenergic innervation with a solid-state dedicated cardiac cadmium-zinc-telluride camera: First clinical experience. Eur Heart J Cardiovasc Imaging 2014;15:575–85.
5. Boogers MJ, Borleffs CJW, Henneman MM, van Bommel RJ, van Ramshorst J, Boersma E, et al. Cardiac sympathetic denervation assessed with 123-iodine metaiodobenzylguanidine imaging predicts ventricular arrhythmias in implantable cardioverter-defibrillator patients. J Am Coll Cardiol 2010;55:2769–77.
6. Flotats A, Carrio I. Cardiac neurotransmission SPECT imaging. J Nucl Cardiol 2004;11:587–602.
7. Podrid PJ, Fuchs T, Candinas R. Role of the sympathetic nervous system in the genesis of ventricular arrhythmia. Circulation 1990;82:I103–13.
8. Jacobson AF, Senior R, Cerqueira MD, Wong ND, Thomas GS, Lopez VA, et al. Myocardial iodine-123 meta-iodobenzylguanidine imaging and cardiac events in heart failure. J Am Coll Cardiol 2010;55:2212–21.
9. Henneman M, Bengel F, Vanderwall E, Knuuti J, Bax J. Cardiac neuronal imaging: Application in the evaluation of cardiac disease. J Nucl Cardiol 2008;15:442–55.
10. Flotats A, Carrió I, Agostini D, Guludec D, Marcassa C, Schaffers M, et al. Proposal for standardization of 123I-metaiodobenzylguanidine (MIBG) cardiac sympathetic imaging by the EANM Cardiovascular Committee and the European Council of Nuclear Cardiology. Eur J Nucl Med Mol Imaging 2010;37:1802–12.
11. Nishisato K, Hashimoto A, Nakata T, Doi T, Yamamoto H, Nagahara D, et al. Impaired cardiac sympathetic innervation and myocardial perfusion are related to lethal arrhythmia: Quantification of cardiac tracers in patients with ICDs. J Nucl Med 2010;51:1241–9.
12. Tamaki S, Yamada T, Okuyama Y, Morita T, Sanada S, Tsukamoto Y, et al. Cardiac iodine-123 metaiodobenzylguanidine imaging predicts sudden cardiac death independently of left ventricular ejection fraction in patients with chronic heart failure and left ventricular systolic dysfunction. J Am Coll Cardiol 2009;53:426–35.
13. Merlet P, Valette H, Dubois-Randé JL, Moyse D, Duboc D, Dove P, et al. Prognostic value of cardiac metaiodobenzylguanidine imaging in patients with heart failure. J Nucl Med 1992;33:471–7.
14. Verberne HJ, Brewster LM, Somsen GA, van Eck-Smit BLF. Prognostic value of myocardial 123I-metaiodobenzylguanidine (MIBG) parameters in patients with heart failure: A systematic review. Eur Heart J 2008;29:1147–59.
15. Agostini D, Carrio I, Verberne HJ. How to use myocardial 123I-MIBG scintigraphy in chronic heart failure. Eur J Nucl Med Mol Imaging 2009;36:555–9.
16. Sood N, Al Badarin F, Parker M, Pullatt R, Jacobson AF, Bateman TM, et al. Resting perfusion MPI-SPECT combined with cardiac 123I-mIBG sympathetic innervation imaging improves prediction of arrhythmic events in non-ischemic cardiomyopathy patients: Sub-study from the ADMIRE-HF trial. J Nucl Cardiol 2013;20:813–20.
17. Du Y, Bhattacharya M, Frey EC. Simultaneous Tc-99m/I-123 dual-radionuclide myocardial perfusion/innervation imaging using Siemens IQ-SPECT with SMARTZOOM collimator. Phys Med Biol 2014;59:2813–28.
18. Esteves FP, Raggi P, Folks RD, Keidar Z, Wells Askew J, Rispler S, et al. Novel solid-state-detector dedicated cardiac camera for fast myocardial perfusion imaging: Multicenter comparison with standard dual detector cameras. J Nucl Cardiol 2009;16:927–34.
19. Slomka PJ, Patton JA, Berman DS, Germano G. Advances in technical aspects of myocardial perfusion SPECT imaging. J Nucl Cardiol 2009;16:255–76.
20. Ogawa K, Harata Y, Ichihara T, Kubo A, Hashimoto S. A practical method for position-dependent Compton-scatter correction in single photon emission CT. IEEE Trans Med Imaging 1991;10:408–12.
21. Ichihara T, Ogawa K, Motomura N, Kubo A, Hashimoto S. Compton scatter compensation using the triple-energy window method for single- and dual-isotope SPECT. J Nucl Med 1993;34:2216–21.
22. Yang JT, Yamamoto K, Sadato N, Tsuchida T, Takahashi N, Hayashi N, et al. Clinical value of triple-energy window scatter correction in simultaneous dual-isotope single-photon emission tomography with 123I-BMIPP and 201Tl. Eur J Nucl Med 1997;24:1099–106.
23. Hesse B, Tägil K, Cuocolo A, Anagnostopoulos C, Bardiés M, Bax J, et al. EANM/ESC procedural guidelines for myocardial perfusion imaging in nuclear cardiology. Eur J Nucl Med Mol Imaging 2005;32:855–97.
24. Cerqueira MD, Weissman NJ, Dilsizian V, Jacobs AK, Kaul S, Laskey WK, et al. Standardized myocardial segmentation and nomenclature for tomographic imaging of the heart. A statement for healthcare professionals from the Cardiac Imaging Committee of the Council on Clinical Cardiology of the American Heart Association. Int J Cardiovasc Imaging 2002;18:539–42.
25. Jaszczak RJ, Coleman RE, Whitehead FR. Physical factors affecting quantitative measurements using camera-based single photon emission computed tomography (Spect). IEEE Trans Nucl Sci 1981;28:69–80.
26. Hendel RC, Berman DS, Cullom SJ, Follansbee W, Heller GV, Kiat H, et al. Multicenter clinical trial to evaluate the efficacy of correction for photon attenuation and scatter in SPECT myocardial perfusion imaging. Circulation 1999;99:2742–9.
27. Xiao J, de Wit TC, Staelens SG, Beekman FJ. Evaluation of 3D monte carlo-based scatter correction for 99 mTc cardiac perfusion SPECT. J Nucl Med 2006;47:1662–9.
28. Hutton BF, Buvat I, Beekman FJ. Review and current status of SPECT scatter correction. Phys Med Biol 2011;56:R85–112.
29. Xiao J, de Wit TC, Zbijewski W, Staelens SG, Beekman FJ. Evaluation of 3D Monte Carlo-based scatter correction for 201Tl cardiac perfusion SPECT. J Nucl Med 2007;48:637–44.

30. Holstensson M, Erlandsson K, Poludniowski G, Ben-Haim S, Hutton BF. Model-based correction for scatter and tailing effects in simultaneous (99m)Tc and (123)I imaging for a CdZnTe cardiac SPECT camera. Phys Med Biol 2015;60:3045–63.
31. Kacperski K, Erlandsson K, Ben-Haim S, Hutton BF. Iterative deconvolution of simultaneous ^{99m} Tc and ^{201} Tl projection data measured on a CdZnTe-based cardiac SPECT scanner. Phys Med Biol 2011;56:1397–414.
32. Pourmoghaddas A, Vanderwerf K, Ruddy TD, Wells RG. Scatter correction improves concordance in SPECT MPI with a dedicated cardiac SPECT solid-state camera. J Nucl Cardiol 2014;24:1–10.
33. Rouzet F, Chequer R, Milliner M, Hyafil F, Burg S, Mohammed Saeed D, et al. Clinical evaluation of simultaneous 123I-MIBG/201Tl imaging with cardiac CZT camera. Soc Nucl Med Annu Meet Abstr 2013;54:518.
34. Ben-Haim S, Kacperski K, Hain S, Gramberg D, Hutton BF, Erlandsson K, et al. Simultaneous dual-radionuclide myocardial perfusion imaging with a solid-state dedicated cardiac camera. Eur J Nucl Med Mol Imaging 2010;37:1710–21.
35. Hartikainen J, Kuikka J, Mäntysaari M, Länsimies E, Pyörälä K. Sympathetic reinnervation after acute myocardial infarction. Am J Cardiol 1996;77:5–9.
36. Carrió I, Cowie MR, Yamazaki J, Udelson J, Camici PG. Cardiac sympathetic imaging with mIBG in heart failure. JACC Cardiovasc Imaging 2010;3:92–100.